Influence of lightning on total electron content in the ionosphere using WWLLN lightning data and GPS data

M M Amin [12] **M Inggs** [1] **P J Cilliers** [2]

[1]South African National Space Agency (SANSA) Space Science, P.O. Box 32, Hermanus 7200, South Africa
[2] Department of Electrical Engineering, University of Cape Town, Western Cape, Cape Town 7100,
South Africa

E-mail: cyrusdv92@yahoo.com (M M Amin) mikings@gmail.com (M Inggs) pjcilliers@sansa.org.za (P J Cilliers)

Abstract. An analysis of total electron content (TEC) variations detected over southern Africa has been performed. We included two days with high lightning activity, one day with low lightning activity and one day with a geomagnetic storm. An attempt to obtain a better understanding of lightning as a source mechanism is motivated by the fact that lightning couples energy directly to the mesosphere and lower ionosphere through quasi-electrostatic (QE) and electromagnetic pulsed (EMP) fields and through upward propagating gravity waves that transfer energy from the site of lightning into the ionosphere. Geomagnetic indices, GPS data from six dual frequency GPS reference stations and lightning data from the World-Wide Lightning Location Network (WWLLN) have been used to explore the origin of the TEC variations detected. The analysis reveals periods of TEC variations of $\sim$ 1 TECU on geomagnetically quiet days which correspond to periods of intense lightning activity in the regions. The TEC variations on the days with high lightning activity appear to have more high-frequency TEC variation content than days with low lightning activity.

1. Introduction

Over the past few decades considerable attention has been given to the effects of thunderstorms and the lightning they produce on the middle and upper atmosphere. For example, a statistical study by Davis and Johnson [1] found a correlation between intensification in the sporadic E layer and lightning activity. In addition, modeling of atmospheric gravity waves (AGWs), originating from thunderstorms, has predicted variations in total electron content (TEC) associated with these AGWs of $\pm$7% [2] and other observations [3, 4] indicate gravity wave effects on the ionosphere from tropical and mid-latitude storms. Recent studies by Lay and Shao [5] on the D layer ionosphere ($\sim$ 65–90 km altitude) have shown that AGWs originating from large mesoscale thunderstorms clearly perturb the electron distribution at the lower boundary of the ionosphere. Studies [6, 7] have shown that the most active regions of thunderstorms are over Africa, the Americas and South-East Asia, with the major proportion of lightning occurring over land. This work is motivated by the potential links between thunderstorms and variations in the ionosphere over South Africa as observed through the background TEC variations. The TEC

variation is an indicator of ionospheric variability and can be derived from GPS signals. The TEC variation is also the parameter of the ionosphere that produces most of the effects on GPS signals. Lightning measurement by the World-Wide Lightning Location Network (WWLLN) was used as a proxy to identify regions of intense thunderstorms and the observations through the ionosphere was conducted by analyzing TEC measurements from ground-based dual frequency GPS receivers in regions with different thunderstorm activity levels within South Africa.

2. Data and Method of Analysis

The automatic lightning detector at the South African National Space Agency (SANSA) Space Science in Hermanus and another in Durban, both in South Africa, and several other such detectors distributed across the globe constitute the WWLLN, which logs the incidences of lightning strikes all over the world (http://webflash.ess.washington.edu/). The WWLLN exploits the VLF (3-30 kHz) band term as "sferics" emitted by lightning during the return stroke and employs the Time of Group Arrival (TOGA) described by Dowden et al. [8] to determine the location of each stroke. Each lightning stroke location requires the TOGA from at least four stations with time residual of less than 30 microseconds [9, 10]. The WWLLN currently has over 50 sensors distributed across the globe and provides real-time lightning locations globally [11] with less than 10 km and 10 microseconds location and timing errors respectively [12].

The ionospheric data (TEC) presented in this study were derived from RINEX file which contains data obtained from six GPS receiver stations belonging to the Trignet (http://www.trignet.co.za/) network. The GPS_TEC software developed at Boston College [13] was used to process the RINEX files to derive the integrated electron density along the signal path between the receiver on the ground and the GPS satellite in space, commonly referred to as slant TEC (STEC). The STEC is calculated at an Ionospheric Pierce Point (IPP) altitude of 350 km with an elevation mask of 15° over the mid-latitude stations. The GPS_TEC software uses the phase and code values for both L1 and L2 GPS frequencies to eliminate the effect of clock errors and tropospheric water vapor to calculate relative values of STEC [14]. To obtain the absolute TEC values, the differential satellite biases (published by the University of Bern) are included along with the receiver bias values that are calculated by minimizing the TEC variability between 02:00 and 06:00 local time [15]. The biases in the observed STEC are accounted for by computation via the expression below.

$$(STEC)_{desired} = STEC + B_{Rx} + B_{Rich} + B_{sat} \tag{1}$$

where B_{Rx}, B_{Rich} and B_{sat} are the receiver bias, receiver inter-channel bias and satellite biases respectively. In order to minimize the multipath effects on GPS data, an elevation cutoff of 20° was applied in selecting data for the analysis. In the method adopted here, the control curves or "undisturbed" conditions (TEC_{fit}) used are modeled by fitting a 6th order polynomial to the STEC measurements by a GPS pseudo-random number (PRN) from each station, similar to the method described in Lay et al. [16]. The degree of variations in the STEC was estimated by subtracting the TEC_{fit} values from the STEC. The removal of the TEC_{fit} tends to filter out lower-frequency variations, hence this method is only sensitive to higher-frequency variation. Geomagnetic activity was expressed in terms of the global geomagnetic index (Kp).

3. Results

The normalized global lightning data from the WWLLN are used to map intense thunderstorm regions over Southern Africa with high time and spatial resolution. The lightning data was recorded in universal time (UT) system per event which is equivalent to South Africa standard time (SAST) (UT + 2 hours).

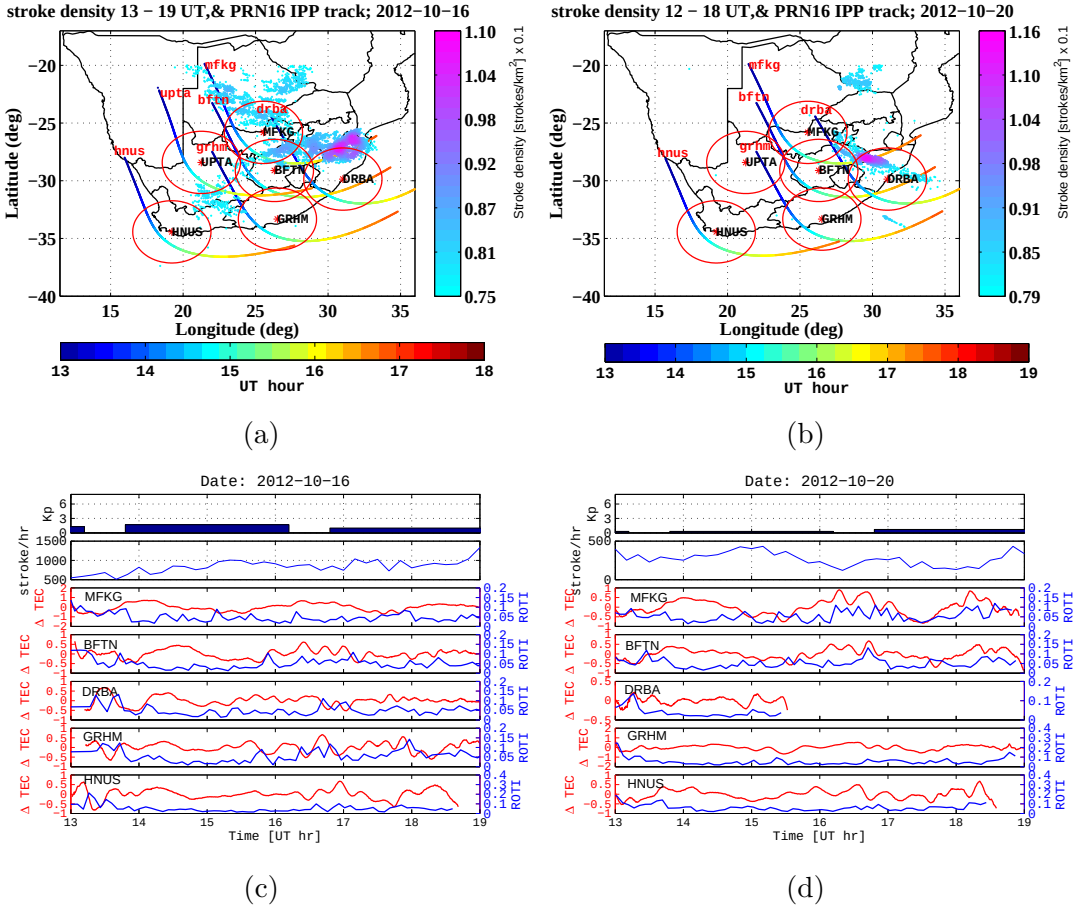

Figure 1: Top row: corresponding TEC measurement paths (Ionospheric Pierce Point (IPP) at 350 km) from PRN 16 between 13:00 and 19:00 UT visible at individual reference receiver stations for high lightning activity and geomagnetically quiet days (a) 16 October,2012 and (b) 20 October, 2012. The rainbow colored curves in (a) and (b) indicate the measuring path of the GPS satellite (PRN-16). The color of the paths is the corresponding time in UT as shown in the colorbar below the figure. The red ellipses indicate 300 km radius around each GPS station. The distribution of stroke/km^2 is also presented in color scale (from light blue to violet):The light blue color indicates regions of relative low stroke/km^2 and the violet color indicates regions of relative high stroke/km^2. Bottom rows: Kp index, stroke rate, STEC variations (Δ TEC) and ROTI for PRN 16, (c) on 16 October,2012 and (d) on 20 October, 2012.

GPS data from six reference GPS receiver stations between 13:00 and 19:00 UT on 5, 8, 16 and 20 October, 2012 has been selected, processed and analyzed and the results to be presented in Figures 1 and 2. The STEC obtained from the GPS_TEC algorithm is used to derived the rate of change of TEC (ROT) and ROT index (ROTI). The ROTI, which can be used as a proxy for the S_4 amplitude scintillation index (S_4p) is defined as the standard deviation over a 5-minute period of ROT calculated from 30-second sampled GPS data [17].

Figure 1, shows that the significant thunderstorm activity which occurred on 16 October, and 20 October 2012 correspond to enhanced TEC variations along the ray path for satellite PRN 16. Although 16 October day has relatively low geomagnetic activity (Kp = 2.3), it has a very active thunderstorm that sustained lightning rates of $>$ 1000 per hour from 13:00 UT to 19:00 UT. The maximum lightning density was $\sim 0.11/\text{km}^2$ located at about 300 km to the north of DRBA Figure 1(a). The ionosphere over South Africa is significantly disturbed during this period as measured by the GPS stations BFTN, DRBA, GRHM, MFKG and HNUS from PRN 16 Figure 1(c).

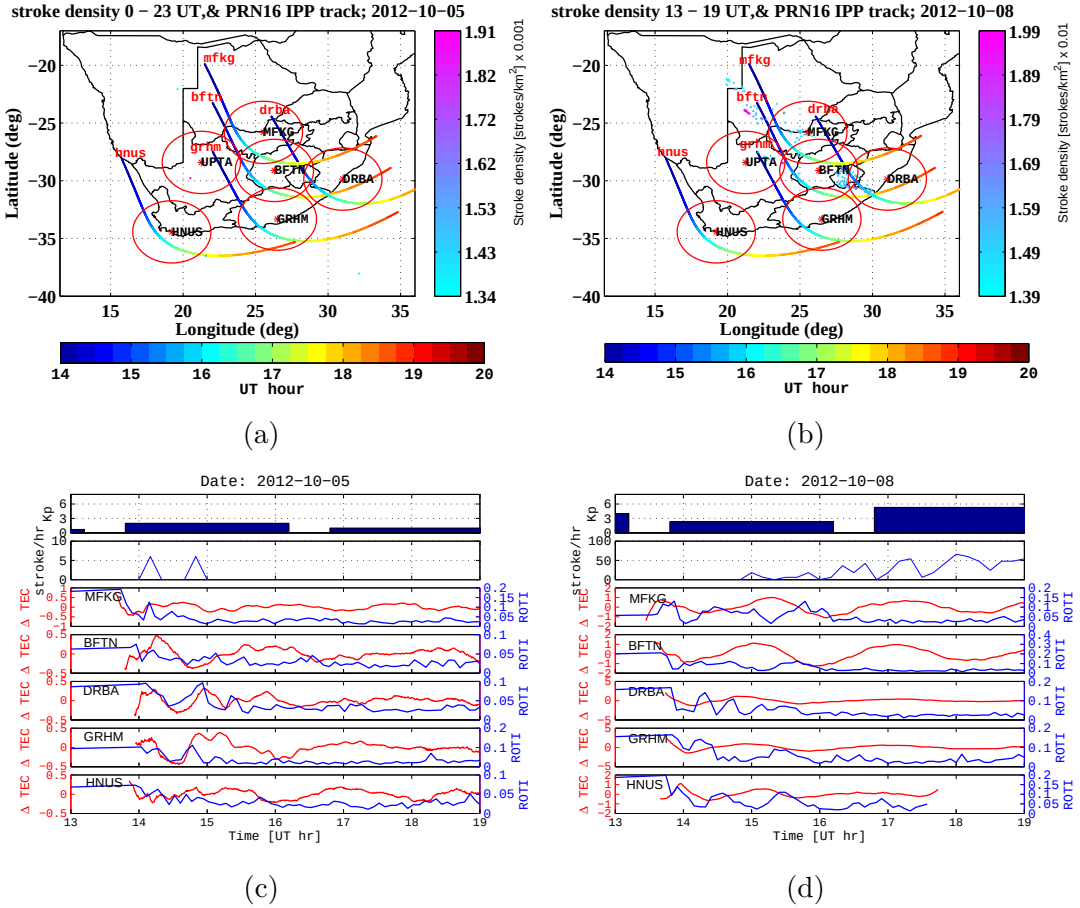

Figure 2: Top rows:corresponding TEC measurement paths (IPP at 350 km) from PRN 16 between 13:00 and 19:00 UT on (a) 5 October, 2012 and (b) 8 October, 2012. Bottom row: Bottom rows: Kp index, stroke rate, STEC variations (Δ TEC) and ROTI for PRN 16 on (c) 5 October, 2012 and (d) 8 October, 2012

October 20 has mach less geomagnetic activity (Kp = 0.7) and a thunderstorm with a relatively higher lightning activity ($\sim 0.116/\text{km}^2$) in a fairly concentrated area within 300 km radius of DRBA. The lightning rate is relatively low (< 500 per hour) between 13:00 UT and 21:00 UT. Enhanced TEC variations also occurred as measured by the above mentioned GPS stations from PRN 16 during the same period when the thunderstorm is active. On 08 October, due to enhanced geomagnetic activity (Kp = 6.3), the TEC variation is larger as measured by GPS stations BFTN, DRBA, GRHM, MFKG, HNUS from PRN 16. Again no data is available from UPTA from PRN 16. On 05 October 2012 there was much less lightning activity ($\sim 0.0019/\text{km}^2$) as shown in Figure 2(b) than on the other three days, and there are no clear enhanced TEC variations as observed by the GPS stations from PRN 16 (Figure 2(d)).

It is interesting to note that the ΔTEC variations on the thunderstorm-active days (Figure 1(c) and Figure 1(d)) have more high-frequency TEC variation contents superimposed on low-frequency background TEC variation than the thunderstorm-quiet (Figure 2(c)) and geomagnetic-active (Figure 2(d)) days.

4. Discussions and conclusions

There is evidence [18] for multiple mechanisms by which lightning can enhance the ionospheric ionization. Our analysis show evidence of lightning related perturbations in ionospheric TEC in the range of 0.5 to 1.2 TECU on selected days when there was high lightning activity and low geomagnetic activity. The mechanism responsible for the perturbations detected

on the thunderstorm-active days is not clear at this stage. Some plausible mechanisms of the perturbations could be: propagating atmospheric gravity waves [1], vertical electrical discharge (such as sprites) [19, 20, 21], AGWs produced when convective thunderstorm activity overshoots the tropopause [22, 2], thunderstorm-produced atmospheric density bubbles [23], or thunderstorm-triggered Perkins instabilities [24] or by a combination of these mechanisms. Wilson [25] also speculated that the ionospheric electric field generated by a large rain cloud may be sufficient to induce ionization at ionospheric altitudes without lightning. Mechanisms involving electrical discharge and infrasonic waves would enhance the ionosphere directly above while atmospheric gravity waves launched by lightning [26, 27] have a very small vertical component and would need to propagate several hundred kilometers horizontally before reaching ionospheric altitudes.

The peak-to-peak magnitude of the ΔTEC variation along the measurement paths (i.e., $bftn$ and $mfkg$) in Figure 1(d) is about 1 TECU on the thunderstorm-active and low geomagnetic-active (i.e Kp = 0.7) day. In comparison, numerical simulations studies have suggested that density perturbations of the order of 5% or even less, attributed to atmospheric gravity waves, can trigger instability growth in the ionosphere leading to vertical development of bubbles to the topside ionosphere under the typical dynamic state of the background ionosphere during the sunset period [28]. In addition Vadas and Liu [2] reported 5% TEC variation due to AGWs generated by a convective plume 1-1.5 h before sunset. Based on the International Reference Ionosphere [29], a typical pre-sunset background of $\sim$ 40 TECU is inferred for the general geographical location. Therefore, a 5% change implies a 2 TECU variation. The result obtained in this paper (1 TECU) and that inferred from Vadas and Liu [2] (2 TECU) could be considered comparable. This discussion presents some individual possibilities for the cause of these TEC perturbations, but it is also possible that multiple mechanisms simultaneously affect the ionosphere above thunderstorms, leading to even more complex coupling dynamics. The fact that there is no noticeable TEC perturbation for geomagnetic-quiet (05 October, 2012) day without lightning is evidence that lightning is necessary for the enhanced TEC perturbation on the thunderstorm-active days (16 and 20 October, 2012). We suggest that because the TEC variations typically occur some distance from the region where the lightning activity is the largest confirms the hypothesis that the enhanced TEC variations is likely due to propagating atmospheric gravity waves that transfer energy from the site of lightning into the ionosphere, or vertical electrical discharge, or by a combination of these two mechanisms. Future data analysis and modeling efforts are needed to understand the possible mechanisms associated with the TEC perturbation.

Acknowledgments

The lightning data used in this work is obtained from the World Wide Lightning Location Network through collaborations with research institutions across the globe including South African National Space Agency. The financial assistance of the National Research Foundation (NRF) towards this research is hereby acknowledged.

References

[1] Davis C J and Lo K-H 2005 Lightning-induced intensification of the ionospheric sporadic-E layer, *Nature* **435** 799–801.

[2] Vadas S L and Liu H -l 2009 Generation of large-scale gravity waves and neutral winds in the thermosphere from the dissipation of convectively generated gravity waves, *J. Geophys. Res.: Space Phys.* **114** A10 doi:10.1029/2009JA014108.

[3] Bishop R L Aponte N Earle G D Sulzer M Larsen M F and Peng G S 2006 Arecibo observations of ionospheric perturbations associated with the passage of Tropical Storm Odette *J. Geophys. Res.: Space Phys.* **111** 1978–2012.

[4] Kelley M C 1997 In situ ionospheric observations of severe weather-related gravity waves and associated small-scale plasma structure, *J. Geophys. Res.: Space Phys.* **102** 329–335.
[5] Lay E H Shao X -M 2011 High temporal and spatial-resolution detection of D-layer variations by using time-domain lightning waveforms, *J. Geophys. Res.: Space Phys.* **116** A1 10.1029/2010JA016018.
[6] Collier A B Hughes A R W Lichtenberger J Steinbach P 2006 Seasonal and diurnal variation of lightning activity over southern Africa and correlation with European whistler observations, *Ann. Geophys.* **24** 529–542.
[7] Lay E H Jacobson A R Holzworth R H Rodger C J Dowden R L 2007 Local time variation in land/ocean lightning flash density as measured by the world wide lightning location network, *J. Geophys. Res.: Atmos.* **112** D13.
[8] Dowden R L Brundell J B Rodger C J 2002 VLF lightning location by time of group arrival (TOGA) at multiple sites *J. Atmos. and Solar-Terres. Phys.* **64** 817–830.
[9] Rodger C J Brundell J B Dowden R L 2005 Location accuracy of VLF World Wide Lightning Location (WWLL) network: Post-algorithm upgrade, *Ann. Geophys.* **23** 277–290.
[10] Rodger C J Brundell J B Dowden R L Thomson N R 2004 Location accuracy of long distance VLF lightning location network *Anna Geophys.* **22** 747–758.
[11] Rodger C J Brundell J B Holzworth R H Lay E H April 2009 Growing Detection Efficiency of the World Wide Lightning Location Network, In *American Inst. Phys. Conf. Series* **1118** 15–20 doi:10.1063/1.3137706.
[12] Abarca S F Corbosiero K L Galarneau T J 2010 An evaluation of the Worldwide Lightning Location Network (WWLLN) using the National Lightning Detection Network (NLDN) as ground truth *J. Geophys. Res.: Atmos.* **115** doi:10.1029/2009JD013411.
[13] Seemala G K Valladares C E 2011 Statistics of total electron content depletions observed over the south american continent for the year 2008, *Radio Sci.* **46** doi:10.1029/2011RS004722.
[14] Sardón E Zarraoa N 1997 Estimation of total electron content using GPS data:How stable are the differential satellite and receiver instrumental biases? *Radio Sci.* **32** 1899–1910.
[15] Doherty P Coster A Murtagh W 2004 Eye on the Ionosphere: space weather effects of October-November 2003 *GPS Solutions* **8** 267–271.
[16] Lay E H Shao X -M Carrano C S 2013 Variation in total electron content above large thunderstorms *Geophys. Res. Lett.* **40** 1945–1949.
[17] Pi X Mannucci A J Lindqwister U J Ho C M 1997 Monitoring of global ionospheric irregularities using the Worldwide GPS Network. *Geophys. Res. Lett.* **24** 2283–2286.
[18] Johnson C G Davis C J 2006 The location of lightning affecting the ionospheric sporadic-E layer as evidence for multiple enhancement mechanisms *Geophys. Res. Lett.* **33** doi:10.1029/2005GL025294.
[19] Neubert, T Rycroft M Farges T Blanc E Chanrion O Arnone E Odzimek A Arnold N Enell C -F Turunen E Bösinger T Mika A Haldoupis C Steiner R Velde O Soula S Berg P Boberg F Thejll P Christiansen B Ignaccolo M Fllekrug M Verronen P Montanya J Crosby N 2008 Recent results from studies of electric discharges in the mesosphere *Surveys in Geophys.* **29** 71–137.
[20] Laštovička J 2006 Forcing of the ionosphere by waves from below, *J. Atmos. and Solar-Terr Phys.* **68** 479–497.
[21] Sentman D D Wescott E M Osborne D L Hampton D L Heavner M J 1995 Preliminary results from the Sprites 94 Aircraft Campaign: 1. red sprites *Geophys. Res. Lett.* **22** 1205–1208.
[22] Alexander M J Holton J R Durran D R 1995 The gravity wave response above deep convection in a squall line simulation *J. Atmos. Sci.* **52** 2212–2226.
[23] Kuo C -L Lee L C Hsu R -R Huba J D 2012 Ionosphere density variations and formation of plasma bubbles caused by thunderstorm currents *Eos Trans. AGU*; AGU Fall Meet. Suppl. Abstract AE41A-04.
[24] Perkins F 1973 Spread F and ionospheric currents, *J. Geophys. Res.* **78** 218–226.
[25] Wilson C T R 1925 The electric field of a thundercloud and some of its effects *Proc. Phys. Soc. Lond.* **37** 32-37.
[26] Chimonas G 1971 Enhancement of sporadic E by horizontal transport within the layer *J. Geophys. Res.* **76** 4578–4586.
[27] Shrrstha K 1971 Sporadic-E and atmospheric pressure waves *J. Atmos. and Terr. Phys.* **33** 205–211.
[28] Abdu M A Kherani E A Batista I S de Paula E R Fritts D C Sobral J H A 2009 Gravity wave initiation of equatorial spread F/plasma bubble irregularities based on observational data from the SpreadFEx campaign *Ann. Geophys.* **27** 2607–2622.
[29] Bilitza D McKinnel L -A Reinisch B and Fuller-Rowell T 2011 International reference, ionosphere today and in the future, *J. Geod.* **85** 909–920 doi:10.1007/s00190-010-0427-x.